ACS Biomaterials SCIENCE & ENGINEERING

Article

pubs.acs.org/journal/abseba

Extracellular Matrix Functionalization and Huh-7.5 Cell Coculture Promote the Hepatic Differentiation of Human Adipose-Derived Mesenchymal Stem Cells in a 3D ICC Hydrogel Scaffold

Yan Wang,[†,⊥] Jae-Ho Lee,[†,⊥] Hitomi Shirahama,[†] Jeongeun Seo,[†] Jeffrey S. Glenn,[§,∥] and Nam-Joon Cho*[,†,‡]

[†]School of Materials Science and Engineering, Nanyang Technological University, 50 Nanyang Avenue 639798, Singapore

[‡]School of Chemical and Biomolecular Engineering, Nanyang Technological University, 62 Nanyang Avenue 637459, Singapore

[§]Division of Gastroenterology and Hepatology, Department of Medicine, Stanford University School of Medicine, Alway Building, Room M211, 300 Pasteur Drive, Stanford, California 94305, United States

[∥]Department of Microbiology and Immunology, Stanford University School of Medicine, Fairchild Building, D300, 299 Campus Drive, Stanford, California 94305, United States

Supporting Information

ABSTRACT: In this study, we constructed a microporous hydrogel scaffold with hexagonally packed interconnected cavities and extracellular matrix (ECM)-functionalized interior surface, and systematically investigated the hepatic differentiation of human adipose-derived mesenchymal stem cells (hAD-MSCs) under the influence of three key factors: three-dimensional (3D) geometry, ECM presence, and coculture with hepatocyte-derived cell line. Results confirmed that (i) hepatic differentiation of hAD-MSC is more efficient in a 3D microporous scaffold than in 2D monolayer culture; (ii) the presence of both ECM components (fibronectin and collagen-I) in the scaffold is superior to collagen-I only, highlighting the importance of fibronectin; and (iii) coculture with Huh-7.5 hepatocyte-derived cells promoted liver-specific functions of the hAD-MSC-derived hepatocytes. The optimized differentiation process only took 21 days to complete, a time length that is shorter or at least comparable to previous reports, and more importantly, yielded an albumin production more than 10-fold higher than conventional 2D culture. Our approach of optimizing hAD-MSC hepatic differentiation could provide a potential solution to the challenges such as hepatocyte transplantation or the establishment of human physiologically relevant liver models *in vitro*.

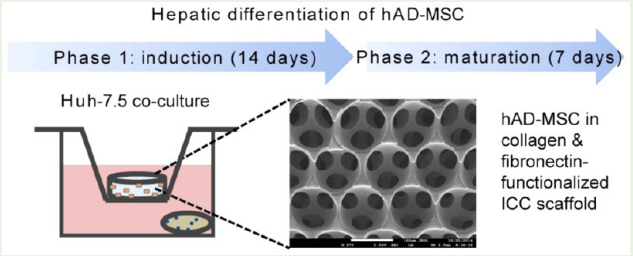

KEYWORDS: *adipose-derived mesenchymal stem cell, hepatocyte, differentiation, extracellular matrix, coculture, 3D culture*

INTRODUCTION

Liver transplantation is currently the only effective treatment for patients with end-stage chronic liver disease and severe liver damage. However, the shortage of organ donors has created long waiting lists, limiting the clinical benefits of this therapy.[1] To fill the growing gap between the availability of, and demand for, organs, various cell-based therapies, including hepatocyte transplantation and artificial liver devices, are being developed in laboratories worldwide in the hope of circumventing the liver supply shortage. Primary hepatocytes are considered to be the optimal choice for cell transplantation; however, these cells proliferate poorly, and they quickly lose their functionality in culture.[1] Drug toxicity and metabolism testing using hepatocytes cultured *in vitro* as liver models are gaining popularity in the pharmaceutical industry.[2,3] Various types of stem cells can be induced to differentiate *in vitro* into hepatocyte-like cells, representing a promising cell source for hepatocyte transplantation therapy, artificial liver devices, and the construction of *in vitro* liver models for drug screening.[4,5]

Studies have revealed a wide range of stem cells that can undergo differentiation into hepatocyte-like cells after appropriate stimulation, including embryonic stem cells (ESCs),[6,7] adult mesenchymal stem cells (MSCs),[4] and induced pluripotent stem cells (iPSCs).[8] While many ethical controversies still surround the use of ESCs and the generation of iPSCs requires a laborious and lengthy induction and selection process, MSCs can be obtained from the bone marrow or adipose tissue of patients. Using autologous MSCs for cell transplantation therapy eliminates the risk of immune rejection and the need for immunosuppression therapy. Adipose-derived MSCs (AD-MSCs) can be harvested in larger quantities using a

Received: August 21, 2016
Accepted: October 19, 2016
Published: October 19, 2016

DOI: 10.1021/acsbiomaterials.6b00487
ACS Biomater. Sci. Eng. 2016, 2, 2255−2265

less invasive procedure that causes less harm to the human body than the harvesting of bone marrow MSCs (BM-MSCs). Additionally, AD-MSCs have a higher proliferation capacity than BM-MSCs.[9,10] Therefore, AD-MSCs have been suggested as an ideal source of stem cells for differentiation into hepatocytes.[9,11−14]

Research on MSCs has been focused on mimicking natural microenvironmental cues that control the differentiation and activity of stem cells.[4] These cues are highly specific and depend on the tissue types. Therefore, providing a mechanical (stiffness),[15] interfacial,[16] and topographical environment[17] that mimics the native tissue may influence the probability of stem cells going through directional differentiation and provides a means to modulate cellular activity in addition to the conventional approach of supplementation with key cytokines and growth factors.[18]

A plethora of studies have been carried out on various factors that affect the hepatic differentiation of stem cells,[19] including the effect of three-dimensional (3D) culture in scaffold systems,[20−23] the composition of the extracellular matrix (ECM),[24−26] and coculture with different types of cell,[26−29] but few have tried to combine these factors and optimize the combination. In the current study, we have successfully induced the differentiation of hAD-MSCs into hepatocyte-like cells by culturing them in an ECM-functionalized 3D microporous scaffold with tunable stiffness while coculturing with hepatocyte-like cells (Huh-7.5) in the presence of appropriate cytokines and growth factors. The synergistic effects of the 3D culture, the presence of ECM, and the coculture with Huh-7.5 cells were confirmed by examining the morphology, cell proliferation, gene and protein expression, and hepatic functionality during and after the differentiation process. This approach holds great promise for potential applications in cell transplantation therapy and the development of liver models *in vitro*.

MATERIALS AND METHODS

Preparation and Characterization of Inverted Colloidal Crystal Scaffolds. The detailed procedure of inverted colloidal crystal (ICC) scaffold construction has been described in an earlier publication.[30] In summary, a prepolymer solution was prepared by dissolving 50% (w/v) PEG-diacrylate (Sigma-Aldrich, MO), 10% (w/v) acryloyl-PEG-*N*-hydroxysuccinimide (NHS) (Laysan Bio, AL), and 0.05% (w/v) photoinitiator 2-hydroxy-4′-(2-hydroxyethoxy)-2-methylpropiophenone (Sigma-Aldrich) in deionized water. Centrifugation allowed the prepolymer solution to infiltrate the polystyrene (PS) colloidal crystal mold, which was then irradiated with 365 nm ultraviolet light (10.84 mW/cm^2) for 5 min to form the hydrogel scaffold. The PS spheres were removed by soaking the scaffold in tetrahydrofuran for 24 h, and then by sequentially washing with 70% ethanol and phosphate buffered saline (PBS; pH 7.4). Subsequently, collagen type I (Sigma-Aldrich) was chemically conjugated to the interior surface of the PEG-NHS scaffold via the cross-linking reaction between the NHS-ester and the free amino groups on the collagen proteins. Three different concentrations of collagen I (20, 200, and 400 μg/mL) were tested for the coating. The 200-μg/mL collagen I coating was determined to be optimal (see Supporting Information Figures S1 and S2). The ICC scaffold coated with 200 μg/mL collagen I (ICC-Col-200) could be further coated with fibronectin via the well-known interaction between fibronectin and collagen,[31] by incubating the scaffold with 10 μg/mL fibronectin at 37 °C for 2 h.

The morphology of the ICC scaffold was observed using scanning electron microscopy (SEM). To prepare the SEM samples, the scaffold was serially dehydrated in ethanol solution and stored at −80 °C until the ethanol completely evaporated. The sample was further dried in a FreeZone 4.5 L freeze-dryer (Labconco, MO) for 48 h and then coated with a 10-nm-thick platinum film on a JFC-1600 sputter coater (JEOL, Tokyo, Japan). Micrographs of the ICC scaffold were taken with a JSM-7600F FE-SEM instrument (JEOL) at a voltage of 5 kV.

Confocal microscopy was used to visualize the fluorescence-stained collagen I and fibronectin coating on the ICC scaffold. The ICC scaffold was washed with PBS, fixed with 4% paraformaldehyde (Alfa Aesar, Ward Hill, MA), and washed again with PBS. The scaffold was then incubated in 3% bovine serum albumin (BSA) at 4 °C overnight with goat anticollagen I primary antibody (Abcam, Cambridge, U.K.) and mouse antifibronectin primary antibody (Abcam). After incubation, the sample was washed with PBS, and then incubated with antigoat secondary antibody conjugated with Alexa Fluor 488 (Life Technologies, Woburn, MA) and antimouse secondary antibody conjugated with Alexa Fluor 555 simultaneously for 2 h (Life Technologies). Fluorescence images of the ICC scaffold were taken on a Carl Zeiss LSM710 confocal microscope coupled with the ZEN program.

Culture of Human Adipose-Derived Mesenchymal Stem Cells. The hAD-MSCs were purchased from ATCC (Manassas, VA). The cells were maintained in MSC basal medium (ATCC), supplemented with a growth kit (ATCC), 100 U/mL penicillin, and 100 μg/mL streptomycin (Life Technologies), and incubated at 37 °C in a humidified atmosphere with 5% carbon dioxide. The culture medium was changed every 3 days, and the cells were subcultured when 80% confluency was reached. Prior to cell seeding, the hAD-MSCs were trypsinized and resuspended in complete growth medium at a concentration of 8×10^5 cell/mL. A total of 2×10^4 cells in a 25-μL cell suspension were pipetted onto each ICC scaffold. After 2 h, the ICC scaffolds were transferred to a new 24-well plate, and the culture medium was changed every 3 days.

Hepatic Differentiation of Human Adipose-Derived Mesenchymal Stem Cells. The basal medium for hepatic differentiation was composed of Iscove's modified Dulbecco's medium (IMDM; Invitrogen, Carlsbad, CA), 10% fetal bovine serum (Hyclone, Logan, UT), 100 U/mL penicillin, and 100 μg/mL streptomycin. A modified two-step protocol[14] was followed to induce the trans-differentiation of hAD-MSCs into hepatocytes. In the induction phase, hAD-MSCs were cultured in the basal medium supplemented with 1 μM hydrocortisone, 0.5 mg/mL BSA, 2 mM ascorbic acid, 5 mM nicotinamide, 10 nM dexamethasone, 100 ng/mL hepatocyte growth factor (HGF), 100 ng/mL fibroblast growth factor (FGF)-1, 10 ng/mL FGF-4, and ITS premix (Invitrogen; final concentration: 10 μg/mL insulin, 5.5 μg/mL transferrin, 40 nM sodium selenite) for 14 days. In the maturation phase, the cells were cultured in the basal medium supplemented with 10 ng/mL HGF, 30 ng/mL oncostatin M (OsM), and 20 μM dexamethasone for 7 days. Hepatic differentiation was assessed through the observation of morphology, functional analysis, and the analysis of specific protein and gene expression.

Coculture of Human Adipose-Derived Mesenchymal Stem Cells with Huh-7.5 Cells. The coculture of hAD-MSCs with Huh-7.5 human hepatocellular carcinoma cells was performed by placing cell culture inserts with 3.0-μm pores (SPL Life Sciences) in 24-well plates. The hAD-MSC-laden ICC scaffolds were placed in the insets, while Huh-7.5 cells were cultured at the bottom of the well. Huh-7.5 cells cultured in 3D collagen hydrogels have previously been proven to be superior to 2D cultures in terms of the expression of hepatic functional proteins (see Supporting Information Figure S3). Therefore, hAD-MSCs were cocultured with Huh-7.5 cells encapsulated in collagen hydrogels. The encapsulation of Huh-7.5 cells in the collagen hydrogels was performed according to a previously published method.[32] A fresh batch of Huh-7.5 cells was used to replace the old batch every 3 days during the coculture with hAD-MSCs and the differentiation process.

Cell Proliferation and Viability. Cell proliferation and viability were quantified using a cell counting kit-8 assay (CCK-8; Dojindo Molecular Technologies, Rockville, MD) according to the manufacturer's protocol. CCK reagent was diluted 10 times with culture media and incubated with cells for 2 h at 37 °C. The supernatant medium was transferred to a 96-well plate, and the absorbance was measured at 450 nm with an Infinite 200 PRO microplate reader (Tecan).

DOI: 10.1021/acsbiomaterials.6b00487
ACS Biomater. Sci. Eng. 2016, 2, 2255−2265

Table 1. Primer Sequences Used in PCR

target gene	forward (5′−3′)	reverse (5′−3′)
ALB	CTGCACAGAATCCTTGGTGA	CTCCTTATCGTCAGCCTTGC
AFP	TCTTTGGGCTGCTCGCTATG	ATGGGCCACATCCAGGACTA
HNF4A	TCGTTGAGTGGGCCAAGTAC	TGTCATCGATCTGCAGCTCC
G6P	TTCCTGTTCAGCTTCGCCAT	TCAAAGACGTGCAGGAGGAC
GAPDH	CCATGGGGAAGGTGAAGGTC	CTCGCTCCTGGAAGATGGTG

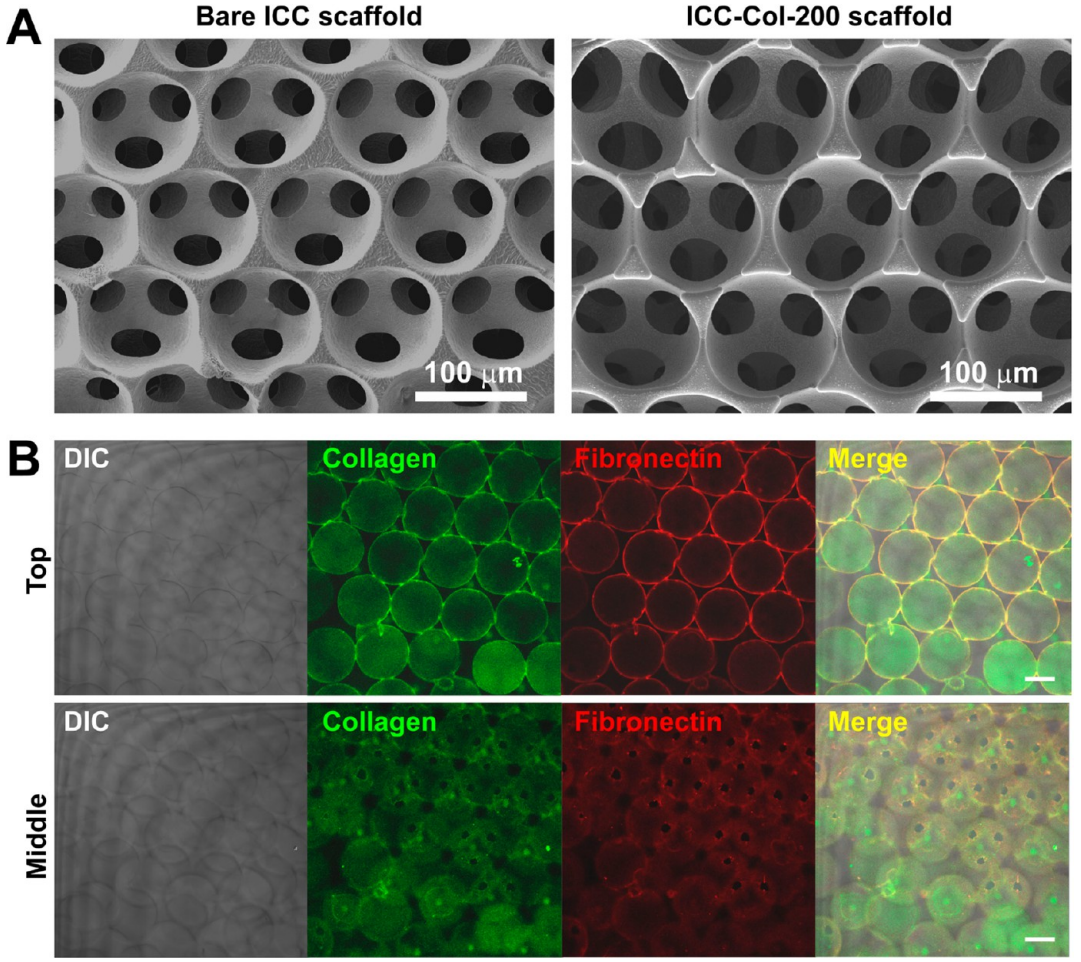

Figure 1. Characterization of ICC scaffolds. (A) SEM images of the ICC scaffold before (left) and after (right) collagen coating. The ICC scaffold was coated with 200 μg/mL collagen I. (B) Immunofluorescence staining of collagen I and fibronectin coated on the interior surface of the ICC scaffold. The scaffold was functionalized with 200 μg/mL collagen I and then 10 μg/mL fibronectin. Results shown are the top and middle sections of differential interference contrast (DIC), collagen (green), fibronectin (red), and merged images. Scale bar is 100 μm.

Cell viability was also assessed using the LIVE/DEAD Viability/Cytotoxicity kit (Life Technologies). To stain the cells, 3 μM calcein acetomethoxy (AM) derivative and 9 μM ethidium homodimer-1 (EthD-1) were prepared in complete cell culture media, added to the cells, and incubated for 1 h in the dark. Cell-permeant calcein AM entered live cells and was converted to calcein, an intensely fluorescent dye, by intracellular esterase, causing live cells to be stained with green fluorescence. EthD-1 was able to enter dead or dying cells with damaged membranes and bind to nucleic acids with a 40-fold enhancement of fluorescence, but was excluded by the intact plasma membranes of live cells. Therefore, only dead cells were stained with red fluorescence. The stained cells were visualized using an LSM710 confocal microscope.

RNA Extraction, Reverse Transcription Polymerase Chain Reaction, and DNA Gel Electrophoresis. The expression of liver-specific gene markers, such as albumin (ALB), α-fetoprotein (AFP), hepatocyte nuclear 4-α (HNF4A), and glucose 6-phosphate (G6P), was assessed using the reverse transcription polymerase chain reaction (RT-PCR) and DNA gel electrophoresis. On days 7, 14, and 21, cellular total RNA was extracted with the TRIZOL reagent (Ambion, CA), and the RNA concentration was measured with a NanoDrop 2000 (Thermo Scientific). The RNA sample was reverse-transcribed to cDNA with SuperScript II reverse transcriptase (Invitrogen) following the manufacturer's instructions. Reverse transcription was performed at 45 °C for 50 min and then at 95 °C for 5 min. The amplification was conducted by a 10 min incubation at 95 °C, followed by 28 cycles at 95 °C for 15 s and 60 °C for 10 min. The PCR products were analyzed using 2% agarose gel electrophoresis, and the gel was imaged with a G:BOX F3 (Syngene). A band intensity analysis was conducted with ImageJ software. The primers (listed in Table 1) were designed using an online primer design program.[33] The band intensity of detected genes was normalized to the GAPDH band intensity.

Western Blot. Nestin, a stem cell protein marker, was analyzed on days 3, 7, and 14. Cell adhesion and ECM proteins, including paxillin, focal adhesion kinase (FAK), vinculin, E-cadherin, and laminin, were analyzed on day 14. Hepatocyte functional marker protein albumin

DOI: 10.1021/acsbiomaterials.6b00487
ACS Biomater. Sci. Eng. 2016, 2, 2255−2265

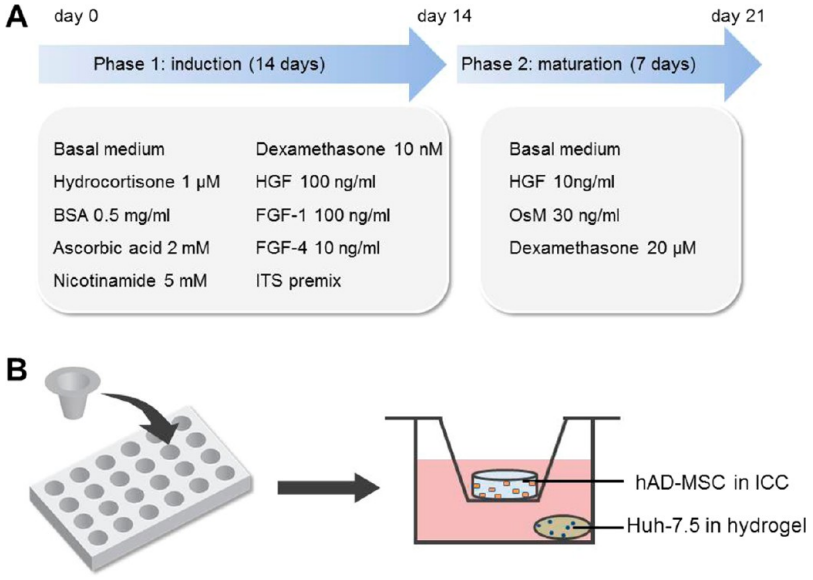

Figure 2. Schema of the experimental design. (A) The induction timeline and composition of the medium for hepatic differentiation of hAD-MSCs. (B) Coculture settings for hAD-MSCs and Huh-7.5 cells in a 24-well plate. The hAD-MSCs were cultured in ICC scaffolds on top of the cell inserts, and Huh-7.5 cells were encapsulated in collagen hydrogel and placed at the bottom of the wells.

was analyzed with Western blot on days 7, 14 (end of the differentiation phase), and 21 (end of the maturation phase). At the indicated time-points, the cells were collected and washed with PBS, resuspended in lysis buffer (Intron Biotechnology), and sonicated for 10 min in iced water. The cell lysates were centrifuged at 15 000 rpm for 30 min, and the supernatant protein solution was collected and stored at −80 °C until analysis. The samples were boiled with 4× Laemmli sample buffer (Bio-Rad, Hercules, CA) for 5 min, and 20 μL of each boiled sample was loaded into wells of an 8% polyacrylamide gel. Sodium dodecyl sulfate polyacrylamide gel electrophoresis was run at 100 V. The proteins were then trans-blotted to a nitrocellulose membrane (Bio-Rad) at 350 mA for 2 h. The trans-blotted membrane was blocked by 5% fat free milk in TBST (pH 7.6 Tris buffer with 0.5% Tween 20) for 1 h at room temperature. The primary antibody (mouse antialbumin (sc-271605), mouse antinestin (sc-23927), mouse antipaxillin (sc-365379), rabbit anti-FAK (sc-557), rabbit antivinculin (sc-5573), rabbit anti-E-Cadherin (sc-7870), rabbit antilaminin (sc-5582), or rabbit anti-GAPDH (sc-25773); Santa Cruz Biotechnology, Santa Cruz, CA) was diluted at a ratio of 1:1000 with 2% fat free milk in TBST solution and incubated with the membrane overnight in a cooled chamber (4 °C). Next, the blotted membrane was washed with 0.5% TBST and incubated with horseradish peroxidase-conjugated antimouse or antirabbit immunoglobulin G secondary antibody (Bio-Rad), depending on the primary antibody used. Immunoreactive bands were detected using an ECL kit (Bio-Rad). The band image and intensity were analyzed using an ImageQuant LAS 4000 mini apparatus (GE Healthcare, Buckinghamshire, U.K.), and the band intensity was normalized to the GAPDH band. All Western blot experiments were performed in triplicate.

Immunofluorescence Staining and Confocal Microscopy. Immunofluorescence staining was also used to assess the cellular albumin levels on days 7, 14, and 21, and the adhesion protein laminin on day 14. The cells were fixed with 4% paraformaldehyde for 5 min, permeabilized with 0.1% Triton X-100 (Bio-Rad) in PBS for 30 min, washed with PBS, and incubated in 3% BSA blocking buffer in PBS for 1 h. The cells were then incubated with the primary antibody overnight at 4 °C in PBS with 1.5% BSA. Afterward, the samples were again washed with PBS, and then incubated with secondary antibody conjugated with fluorescein isothiocyanate (Life Technologies) for 2 h. At the same time, F-actin was stained with Alexa Fluor 555-conjugated phalloidin (Life Technologies). Finally, the cells were counterstained with 300 nM 4′,6-diamidino-2-phenylindole (DAPI; Life Technologies) for 5 min. The fluorescence images were taken on a Carl Zeiss LSM710 confocal microscope.

Functional Assay: Albumin Production and Ammonia Detoxification. Albumin production was assayed on days 14 and 21. The medium of the cells was changed 1 day before the albumin secretion analysis. In the coculture experiments, the cell-laden ICC scaffold was separated from the Huh-7.5 cells 1 day before the assay so that the albumin produced by Huh-7.5 cells would not be detected. The cells were incubated in fresh medium for 24 h, and the secreted albumin concentration in the supernatant medium was analyzed with an enzyme-linked immunosorbent assay kit (Abcam) following the manufacturer's protocol. The results from each group were normalized to the respective cell numbers measured by the CCK-8 assay.

On day 21 (end of the maturation phase), 6 mM ammonium chloride was added to each group of cells and incubated for 24 h. In the coculture experiments, the cell-laden ICC scaffold was separated from the Huh-7.5 cells before the addition of ammonium chloride. After 24 h, the urea concentration in the supernatant medium was analyzed with a colorimetric assay kit (Pars Azmoon) following the manufacturer's protocol. The colorimetric reading was performed on an Infinite 200 PRO microplate reader. The results were normalized to cell numbers measured by the CCK-8 assay.

Statistics. The results presented in the graphs are the means ± standard deviations of triplicate experiments. The data were analyzed by one-way analysis of variance followed by Tukey testing for significant differences between groups. A difference of $p < 0.05$ was considered to be statistically significant.

RESULTS

The ICC scaffolds were constructed with uniform pores approximately 100 μm in diameter (Figure 1A). The surface texture differed before and after the collagen coating, as shown in the SEM images. An optimal concentration of 200 μg/mL for collagen-I coating has been determined and reported previously.[30,34] In this study, the 20-μg/mL level of collagen-I coating was too low, as we saw relatively weak green fluorescence in Figure S1 and low level of cell attachment in Figure S2. At higher collagen-I concentrations, both 200 μg/mL and 400 μg/mL collagen-I coatings have generated similar results, in terms of immunofluorescence staining (Figure S1) as well as cell attachment and viability (Figure S2). On the basis of

DOI: 10.1021/acsbiomaterials.6b00487
ACS Biomater. Sci. Eng. 2016, 2, 2255−2265

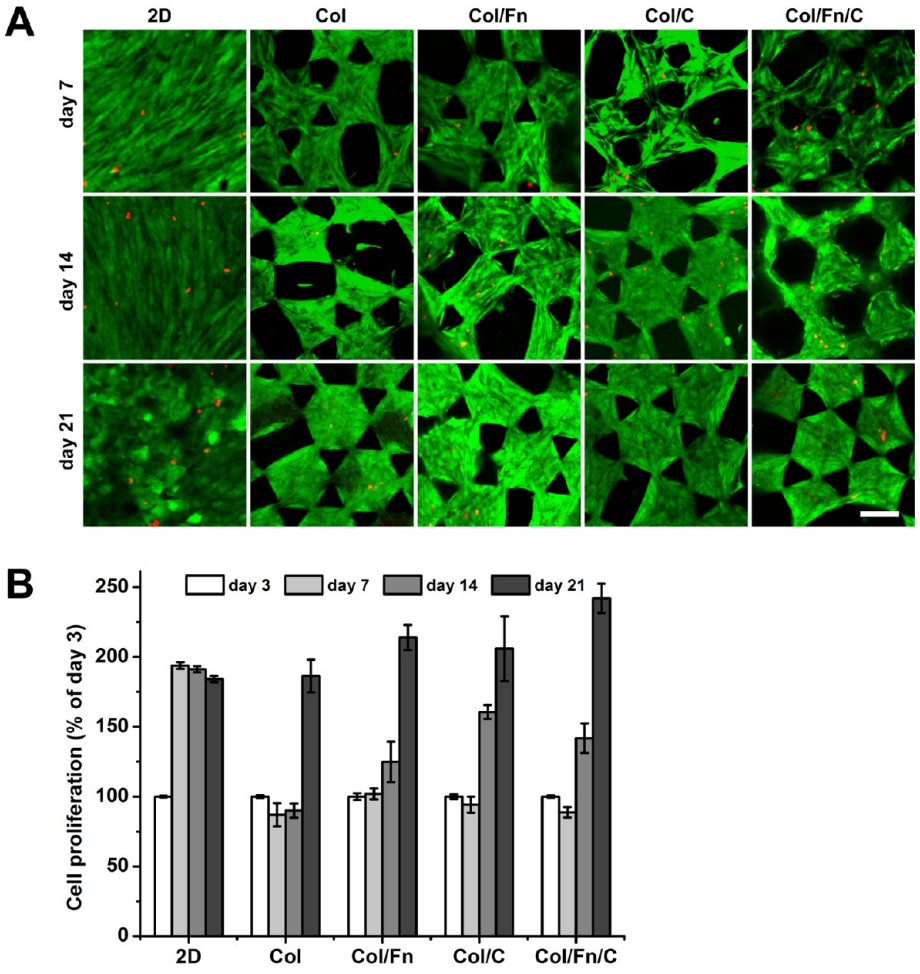

Figure 3. Viability of the cells undergoing differentiation. (A) Live/dead staining of cells at days 7, 14, and 21. Live cells were stained with calcein (green), and dead cells were stained with EthD-1 (red). Images were taken on a confocal microscope with a 20× lens, and the merged images of green and red fluorescence were presented. Scale bar is 100 μm. (B) Cell proliferation under various conditions during the differentiation process. Cell proliferation was quantified by the CCK-8 assay on days 3, 7, 14, and 21, and the results were normalized to the day 3 absorbance values of each respective condition (n = 3, mean ± standard deviation).

the economical consideration, we have chosen to use 200 μg/mL collagen-I to coat the ICC scaffold in the following studies. When ICC-Col-200 was further coated with 10 μg/mL fibronectin, both collagen-I and fibronectin were confirmed by immunofluorescence staining to be present on the interior surface of the scaffold, as evidenced by the even distribution of green and red fluorescence, respectively (Figure 1B).

To study the effect of 3D cell culture, ECM composition, and coculture on the hepatic differentiation of hAD-MSCs, we conducted differentiation under the following five conditions (Figure 2A): (i) 2D monoculture as a control (designated 2D); (ii) hAD-MSC monoculture in a collagen-functionalized ICC scaffold, ICC-Col-200 (designated Col); (iii) hAD-MSC monoculture in a collagen-, then fibronectin-, functionalized ICC scaffold (designated Col/Fn); (iv) hAD-MSC in ICC-Col-200, cocultured with Huh-7.5 cells encapsulated in hydrogel (designated Col/C); and (v) hAD-MSC in a collagen-, then fibronectin-, coated ICC scaffold, cocultured with Huh-7.5 cells encapsulated in hydrogel (designated Col/Fn/C). The differentiation process was optimized on the basis of several reported methods.[14,35,36] Under the optimized conditions (Figure 2B), hepatic differentiation was induced by a mixture of growth factors and small molecules, including HGF, FGF-1, FGF-4, hydrocortisone, ascorbic acid, and nicotinamide. The maturation of hepatocytes occurred in oncostatin M- and dexamethasone-supplemented basal medium.

Cell proliferation and viability during the whole differentiation period were analyzed by calcein AM/EthD-1 cell staining and observation under a confocal microscope (Figure 3A). Live cells were stained with calcein (green fluorescence), while dead cells were stained with EthD-1 (red fluorescence). In all five groups, a majority of the cells were alive with strong green fluorescence throughout the experimental period (21 days), whereas dead cells (the red spots) were scarce. The morphological changes in the cells were clearly demonstrated in 2D culture where the cells exhibited fibroblastic morphology (elongated shape) at day 7, and a polygonal shape (typical morphology of a hepatocyte) after differentiation at day 21. However, because the cells were not located on a single focal plane in 3D culture, it was not as easy to identify the cell shapes in the ICC scaffold as in 2D culture, but the overall morphological changes were still visible. An increase in cell density and cell number was observed from day 7 to day 21. When the cells from the Col, Col/Fn, Col/C, and Col/Fn/C groups were compared, the only difference appeared to be the cell growth rate, with no significant difference in morphology. A quantitative analysis of cell proliferation with the CCK-8 assay (Figure 3B) revealed the different cell growth patterns of the

DOI: 10.1021/acsbiomaterials.6b00487
ACS Biomater. Sci. Eng. 2016, 2, 2255−2265

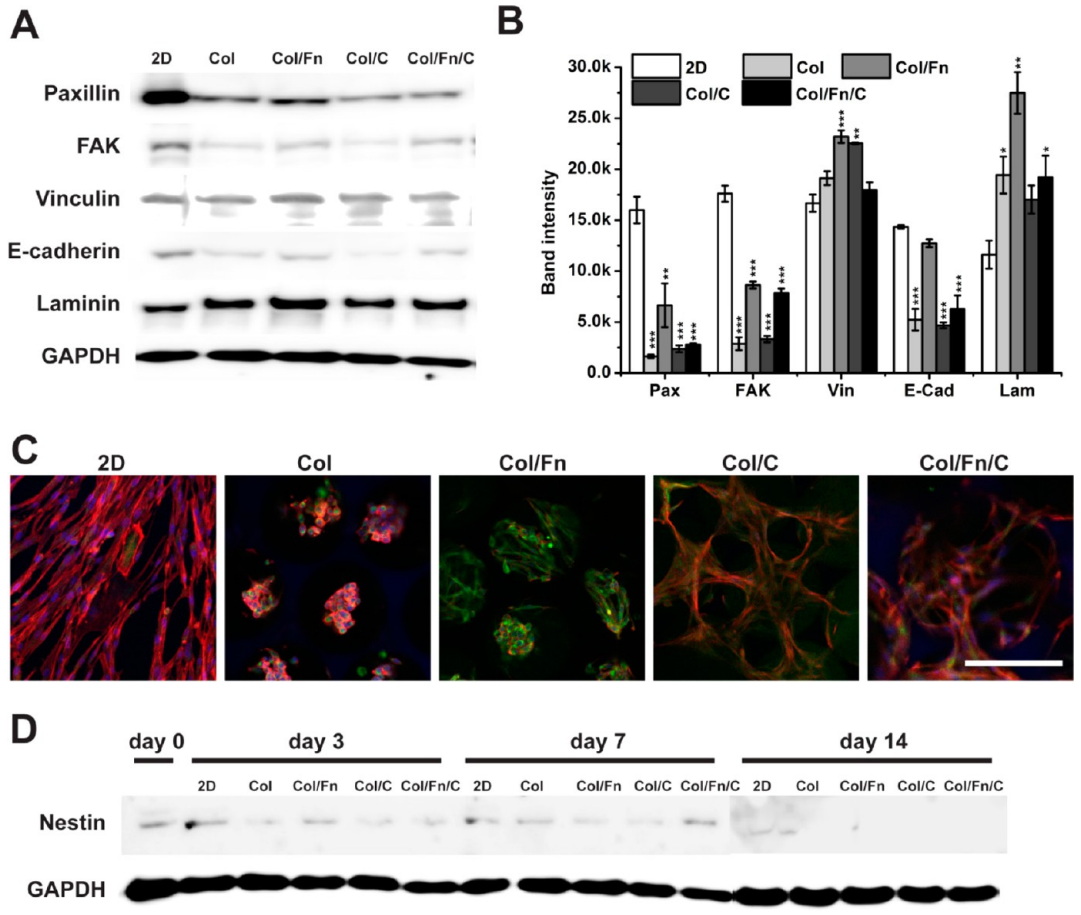

Figure 4. Analysis of protein expression during the differentiation process. (A) Western blot of the cell adhesion proteins paxillin, FAK, vinculin, E-cadherin, and ECM protein laminin on day 14 under 2D and 3D culture conditions. (B) Western blot band intensity of proteins normalized to the respective GAPDH bands (n = 3, mean ± standard deviation); *p < 0.05, **p < 0.01, ***p < 0.001, compared with the band intensity under 2D conditions. (C) Immunofluorescence staining of laminin (green) on day 14; F-actin was stained with phalloidin conjugated with Alexa Fluor 555, and the cell nucleus was counterstained with DAPI. The results presented are merged images of blue, green, and red fluorescence; scale bar, 100 μm. (D) Western blot of the stem cell protein marker nestin from day 0 to day 14.

five groups. Note that the CCK-8 assay measures metabolic activity of the cells, so the changes in absorbance reveal the combined results of changes in cell number and cellular metabolic activity. The absorbance in 2D culture doubled from day 3 to day 7, and remained almost constant from day 7 to day 21, probably due to the space restriction for cell growth, as cells had clearly reached 100% confluency at day 7 (Figure 3A). In the Col group, the absorbance did not increase from day 3 to day 14 during the induction phase, but the absorbance doubled in the maturation phase from day 14 to day 21. In the Col/Fn, Col/C, and Col/Fn/C groups, the cell growth was stagnant from day 3 to day 7; however, the absorbance increased from day 7 to day 21. For all of the 3D culture groups, the drastic increase of absorbance from day 14 to day 21 should be attributed more to the increased metabolic activity during hepatocyte maturation and less to cell proliferation.

To evaluate the effect of 3D culture on cell adhesion markers, we examined the expression of several cell adhesion proteins using Western blot on day 14 (Figure 4A,B). Paxillin, FAK, and vinculin are important proteins involved in cell-matrix adhesion.[37] Cell-matrix adhesions in 3D scaffolds have been suggested to differ vastly from the focal adhesions characterized on 2D substrates in their components.[38,39] We found that the expression of paxillin and FAK in the 3D culture groups was much lower than that in 2D culture, while vinculin expression was slightly higher (Figure 4A,B). We also observed the downregulation of the cell−cell adhesion protein E-cadherin in the 3D culture groups compared with the 2D culture groups, which was consistent with a previous report that the CDH1 gene (encoding E-cadherin) was downregulated in the 3D spheroids of HepG2 hepatocarcinoma cells compared with the 2D monolayers.[40] The 3D culture groups expressed higher levels of laminin, the major component of the basal lamina of the ECM. The level of laminin expression was confirmed by immunofluorescence staining followed by confocal microscopy (Figure 4C). The cells in the 2D cultures expressed relatively low levels of laminin with weak green fluorescence staining, while in the Col, Col/Fn, Col/C, and Col/Fn/C groups, the green fluorescence staining of laminin was significantly stronger. The green fluorescence was strongest in the Col/Fn group, which was consistent with the highest intensity laminin band shown by Western blot (Figure 4A,B). Similar findings were reported by several other groups. For example, Selden et al. reported that laminin protein expression of HepG2 cells was stronger in a 3D spheroid than in monolayer cultures,[41] and Ghosh et al. found that both LAMB3 and LAMA4 genes encoding laminin β 3 and laminin α 4, respectively, were upregulated in multicellular tumor spheroids as compared with monolayer NA8 melanoma cells.[42]

DOI: 10.1021/acsbiomaterials.6b00487
ACS Biomater. Sci. Eng. 2016, 2, 2255−2265

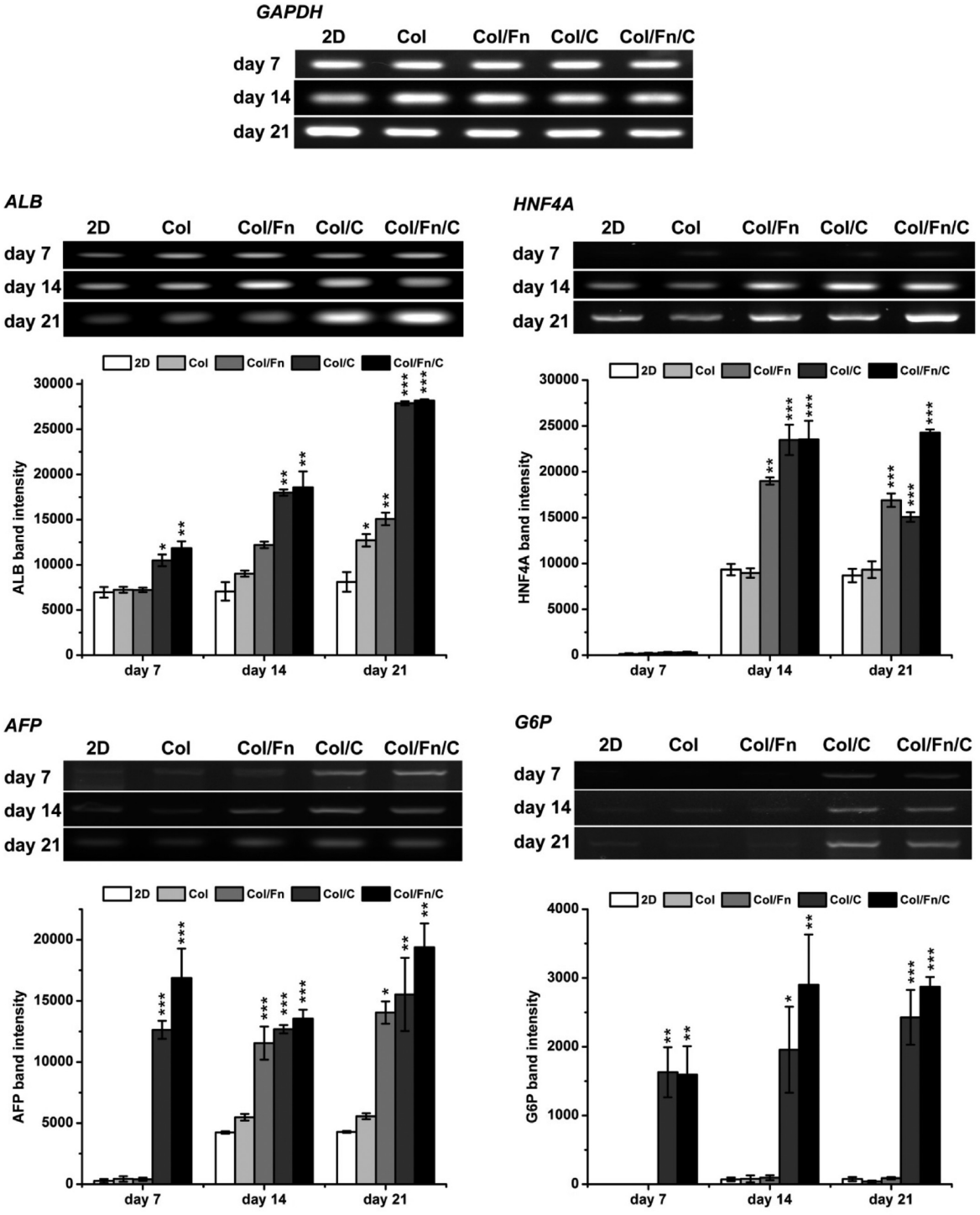

Figure 5. Evaluation of liver-specific gene expression during the differentiation process. RT-PCR and DNA gel electrophoresis were used to analyze the gene expression levels of albumin (ALB), hepatocyte nuclear factor 4 α (HNF4A), α-fetoprotein (AFP), and glucose 6-phosphatase (G6P). The band intensity on the DNA gel was quantified with ImageJ software and normalized to the respective GAPDH band (n = 3, mean ± standard deviation); *p < 0.05, **p < 0.01, ***p < 0.001, compared with the band intensity of the 2D group.

Expression of the stem cell marker nestin[43] from day 0 to day 14 was examined by Western blot (Figure 4D). The nestin band was weak but visible on days 0, 3, and 7 in all five groups, but completely disappeared by day 14 (the end of the induction phase), suggesting that the stem cells in all groups had differentiated at this point regardless of culture conditions.

Next, we evaluated the extent of hepatic differentiation by analyzing the expression of the hepatocyte-specific genes ALB, HNF4A, AFP, and G6P with RT-PCR followed by DNA gel electrophoresis on days 7, 14, and 21 during the differentiation process (Figure 5). GAPDH was used to normalize the band intensity of the genes of interest. We saw a steady increase in ALB gene expression in 3D cultures (Col, Col/Fn, Col/C, and Col/Fn/C groups) from day 7 to day 21, but there was no change in the 2D group during this period. On day 21, ALB gene expression in the coculture groups (Col/C and Col/Fn/

DOI: 10.1021/acsbiomaterials.6b00487
ACS Biomater. Sci. Eng. 2016, 2, 2255−2265

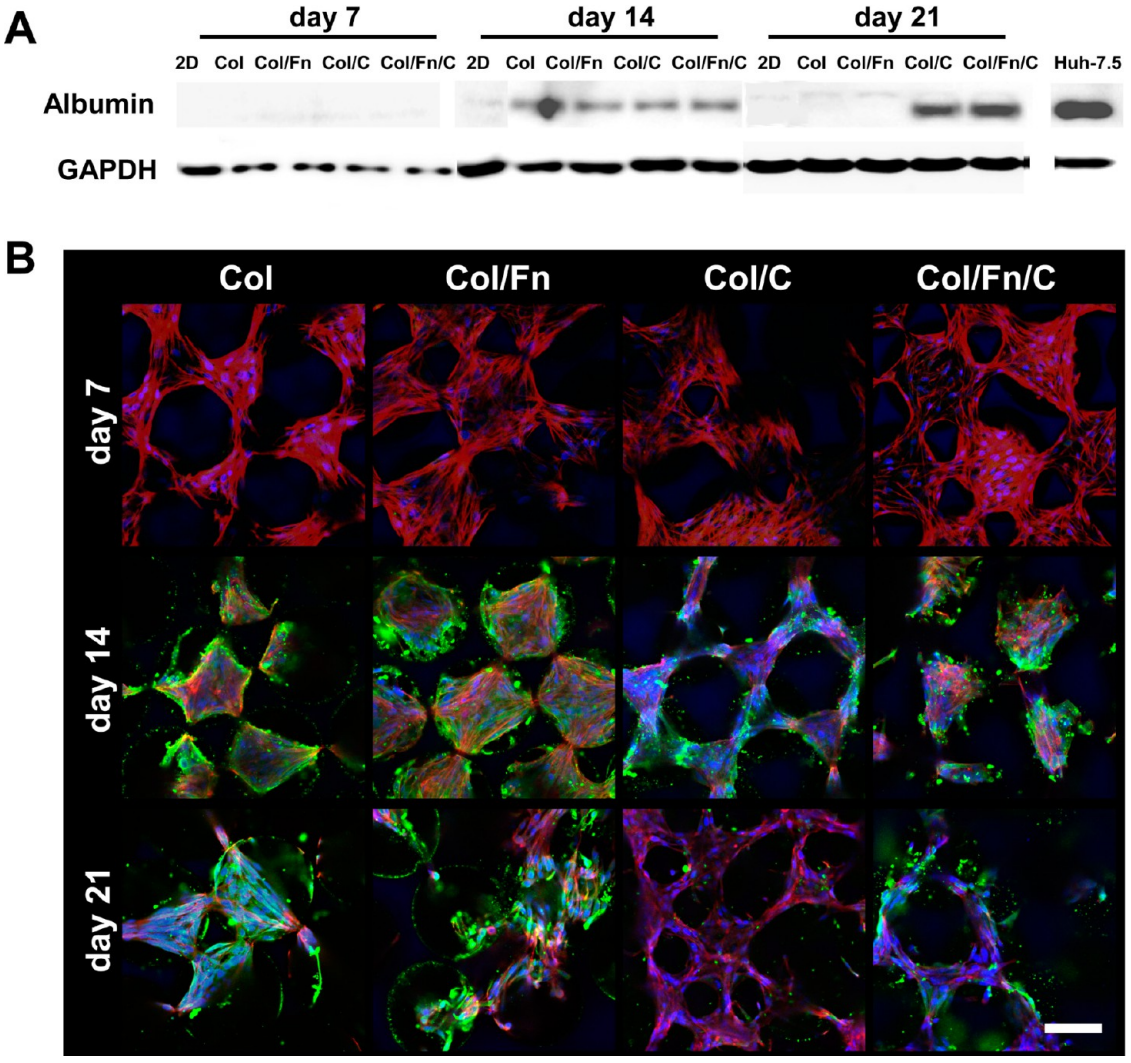

Figure 6. Detection of hepatocyte-specific protein albumin on days 7, 14, and 21 of the differentiation process. (A) Western blot of albumin. Huh-7.5 hepatocarcinoma cells that have a high expression of albumin were used as a positive control. (B) Immunofluorescence staining of albumin. Albumin was stained with a secondary antibody conjugated with fluorescein isothiocyanate (green); F-actin was stained with phalloidin conjugated with Alexa Fluor 555, and the cell nucleus was counterstained with DAPI. The results presented are merged images of blue, green, and red fluorescence. Scale bar, 100 μm.

C) was the highest. An increase in HFN4A and AFP gene expression was observed in all five groups over the experimental period, with the Col/Fn/C group exhibiting the highest level at day 21. Interestingly, the level of AFP gene expression in the 2D Col and Col/Fn groups was still low at day 7, while it was already considerably higher in the Col/C and Col/Fn/C group at day 7. Lastly, G6P expression in the 2D Col and Col/Fn groups was very low even at day 21, while we saw a steady increase in the Col/C and Col/Fn/C groups from day 7 to day 21. The highest level of G6P expression was found in the Col/Fn/C group.

The intracellular level of hepatocyte-specific protein albumin was monitored by Western blot (Figure 6A) and immunofluorescence staining (Figure 6B) during the differentiation process. Huh-7.5 cells were used as a positive control in Western blot as they strongly express albumin. On day 7, no albumin band was visible for any of the groups, but it did appear on day 14, with the 3D culture groups expressing higher levels of albumin than the 2D culture group. By day 21, a strong albumin band was only found in the coculture groups (Col/C and Col/Fn/C), clearly highlighting the positive role of Huh-7.5 coculture on the hepatic differentiation of hAD-MSCs. Similar results were obtained from the immunofluorescence staining images (Figure 6B).

Finally, we conducted a functional assessment of hAD-MSC-derived hepatocytes, including the analysis of albumin production and ammonia detoxification capacity. Albumin production was examined by an enzyme-linked immunosorbent assay on days 14 and 21 (Figure 7A). The level was relatively low in the 2D, Col, and Col/Fn groups at both day 14 and day 21, while albumin production was promoted by coculture conditions (Col/C and Col/Fn/C groups) at day 14 compared with the other groups, increasing to even higher levels by day 21. This was consistent with the results shown in Figure 6. The ammonia detoxification function of hepatocytes at day 21 was assessed by adding ammonium chloride to the cell culture and analyzing urea production after 24 h (Figure 7B). Cells in 3D culture (Col, Col/Fn, Col/C, and Col/Fn/C groups) were able to process ammonia and produce at least twice as much urea as those in 2D cultures. The difference among different 3D culture groups was insignificant.

DOI: 10.1021/acsbiomaterials.6b00487
ACS Biomater. Sci. Eng. 2016, 2, 2255−2265

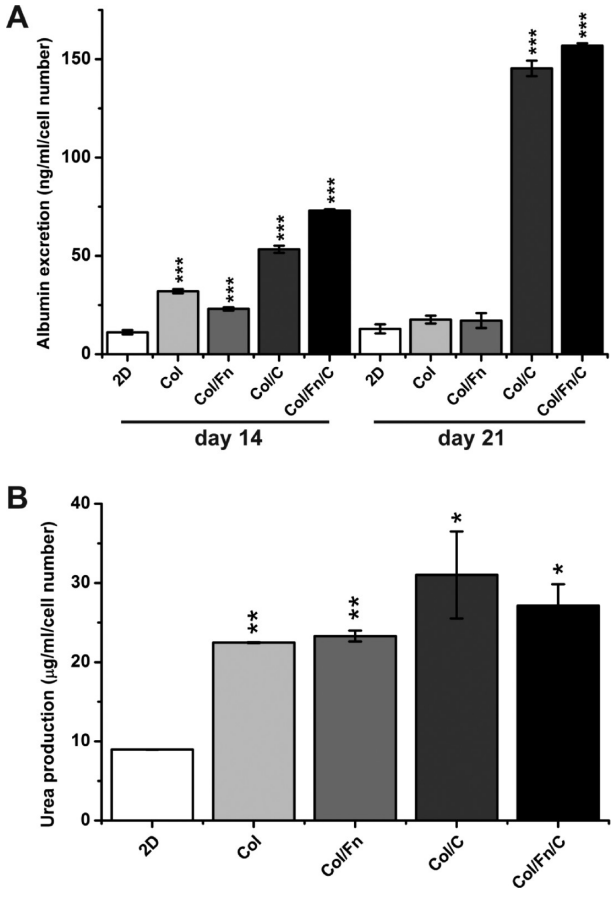

Figure 7. Functional assessment of hAD-MSC-derived hepatocytes. (A) The 24 h excretion of albumin on days 14 and 21 (n = 3, mean ± standard deviation). (B) The ammonia detoxification capacity of cells on day 21 measured by urea production after a 24 h incubation with 6 mM ammonium chloride (n = 3, mean ± standard deviation). Results were normalized to the respective cell numbers measured by the CCK-8 assay; *p < 0.05, **p < 0.01, ***p < 0.001, compared with the 2D group.

DISCUSSION

We have demonstrated in this study that culturing hAD-MSCs in ICC scaffolds has a profound influence on the expression of cytoskeletal, adhesion, and ECM proteins compared with 2D monolayer cultures (Figure 4). Considering the concomitant changes in hepatic cell functionality (Figure 7), we can conclude that the ICC scaffold is an improved 3D culture environment for cells versus 2D growth conditions. Although most reported studies of stem cell differentiation were conducted in 2D monolayer cultures, emerging evidence suggests that 3D culture in scaffold systems can promote the hepatic differentiation and maturation of stem cells. For example, it has been reported that human ESCs forming multilayered colonies on micropatterned wells exhibited enhanced homogeneity and maturation compared with those in conventional 2D formats.[20] Murine iPSCs and ESCs were reported to differentiate into hepatocytes in a 3D microcavitary alginate hydrogel system.[44] Another advantage of 3D cell culture systems over 2D monolayer culture is that they maintain the functionality of the hepatocytes for longer periods of time than 2D cultures.[45] Our results suggested that 3D culture in ICC scaffolds promoted the expression of hepatic functional proteins in hAD-MSC-derived hepatocytes, e.g., albumin at both the gene and protein levels (Figures 5 and 6). In addition, the cells differentiated in 3D culture seemed to possess more of the polygonal morphology, a phenotype resembling primary hepatocytes, compared with the cells in 2D culture (see Figure 3A). These findings are corroborated by a number of recent studies comparing the hepatic differentiation of stem cells in 3D culture and monolayer culture.[21,22,46]

In addition to 3D geographical effects, the ECM interface plays an important role in the regulation of cell adhesion and a cascade of subsequent cell behaviors, including cell proliferation, migration, and differentiation.[47] Therefore, the application of appropriate bioactive scaffolds is imperative for optimizing the differentiation of stem cells. On the basis of the results of our preceding experiments,[30,34] the type I collagen-functionalized ICC platform has appropriate topographic properties and bioactivities for the culture of model liver cells (Huh-7.5) and the maintenance of liver-specific functions. Note that liver ECM contains a number of different types of collagen, including collagen type I, III, IV, V, and VI, and each may have a different pattern of distribution and role in the regulation of hepatocytes.[48,49] We have decided to use just collagen-I, not only because it is widely used by other researchers and therefore well-understood, but also because we want to focus more on the other key factors of this study.

Fibronectin is another important component of ECM with unique properties and functions which differ from those of the collagen family. For instance, Martinez-Hernandez reported that, in normal rat liver, fibronectin was in direct contact with the hepatocytes microvilli, forming a continuous structure, and was the most prominent component of the ECM in Disse's space;[49] Sawada et al. found that fibronectin was most permissive for the hepatocyte DNA synthesis, among other ECM proteins.[50] Also, a study by Sanchez and colleagues revealed the unique role and importance of fibronectin in the regulation of hepatocyte morphology, cell organization, and hepatic gene expression of rat fetal hepatocytes.[51] Therefore, in the current study, we constructed a class of ICC scaffold that was simultaneously functionalized with both collagen and fibronectin and compared it with a collagen-functionalized ICC scaffold. As a result, we proved that the addition of fibronectin to the collagen I in the ECM layer of a biofunctionalized ICC scaffold is beneficial for the hepatic differentiation of hAD-MSCs. The positive effect of fibronectin was most clearly demonstrated in the comparisons of ALB and AFP gene expression in the Col/Fn group with that in the Col group or HNF4A and G6P gene expression in the Col/Fn/C group with that in the Col/C group (Figure 5). Furthermore, the albumin production of the Col/Fn/C group was consistently higher than that in the Col/C group on days 14 and 21 (Figure 7A).

Our results showed that coculturing of hAD-MSCs with Huh-7.5 cells has a promoting effect on the hepatic differentiation of the stem cells. We observed higher hepatic-specific gene expression (Figure 5), higher albumin protein expression (Figure 6), and a stronger capacity for albumin production and ammonia detoxification in coculture groups compared with monoculture groups (Figure 7). Because no direct contact occurred between the stem cells and Huh-7.5 cells, the promoting effect could most likely be attributed to a mixture of growth factors and molecules excreted to the culture media by the Huh-7.5 cells, although the composition of this mixture remains elusive. Similar effects have been documented in a number of studies conducted by other groups.[27−29] For example, Soto-Gutierrez et al. reported that mouse ESCs could

DOI: 10.1021/acsbiomaterials.6b00487
ACS Biomater. Sci. Eng. 2016, 2, 2255−2265

be differentiated to hepatocyte-like cells by coculture with human liver nonparenchymal cell lines (immortalized human cholangiocyte MMNK-1, liver endothelial cell TMNK-1, or hepatic stellate cell TWNT-1).[29] In another study by Baertschiger et al., coculture with Huh-7 cells (a cell line that is very similar to Huh-7.5 cells) promoted albumin expression in human MSC, even in the absence of a hepatogenic differentiation medium that contains HGF, FGF-4, and oncostatin M.[27] Zhang and colleagues showed that the hepatic differentiation of rat MSC was much more successful by coculturing with freshly isolated hepatocytes than those treated with HGF only.[28] Due to the complex nature of liver cell-conditioned medium, none of these studies have explicitly identified the molecules excreted by the cocultured cells that promote hepatic differentiation of stem cells. Nevertheless, on the basis of our results and the observations shown in the references, the cocultured liver cells may have excreted various growth factors such as HGF or FGF-4, and many more unknown components, which will need further investigation in future studies.

CONCLUSIONS

In this study, we have constructed a series of 3D ICC scaffolds with ECM functionalization, and studied the hepatic differentiation of hAD-MSCs in these microporous materials in the presence or absence of cocultured Huh-7.5 cells. The results confirmed the positive effect of 3D culture in an ICC scaffold, the presence of ECM protein (both collagen I and fibronectin), and coculture with Huh-7.5 cells on the hepatic differentiation of hAD-MSCs. This system is worthy of further development for potential application in hepatocyte transplantation therapy or the design of *in vitro* liver models.

ASSOCIATED CONTENT

Supporting Information

The Supporting Information is available free of charge on the ACS Publications website at DOI: 10.1021/acsbiomaterials.6b00487.

Confocal microscope images, live/dead images, and protein expression of Huh-7.5 cells cultured in 2D plates and 3D hydrogels (PDF)

AUTHOR INFORMATION

Corresponding Author

*E-mail: NJCho@ntu.edu.sg.

Author Contributions

⊥Y.W. and J.-H.L. contributed equally to this work.

Notes

The authors declare no competing financial interest.

ACKNOWLEDGMENTS

The authors wish to acknowledge supports from the National Research Foundation Fellowship (NRF-NRFF2011-01) and the Competitive Research Programme (NRF-CRP10-2012-07).

REFERENCES

(1) Lee, S. Y.; Kim, H. J.; Choi, D. Cell sources, liver support systems and liver tissue engineering: alternatives to liver transplantation. *Int. J. Stem Cells* **2015**, *8* (1), 36−47.

(2) Godoy, P.; Hewitt, N. J.; Albrecht, U.; Andersen, M. E.; Ansari, N.; Bhattacharya, S.; Bode, J. G.; Bolleyn, J.; Borner, C.; Bottger, J.; Braeuning, A.; Budinsky, R. A.; Burkhardt, B.; Cameron, N. R.; Camussi, G.; Cho, C. S.; Choi, Y. J.; Craig Rowlands, J.; Dahmen, U.; Damm, G.; Dirsch, O.; Donato, M. T.; Dong, J.; Dooley, S.; Drasdo, D.; Eakins, R.; Ferreira, K. S.; Fonsato, V.; Fraczek, J.; Gebhardt, R.; Gibson, A.; Glanemann, M.; Goldring, C. E.; Gomez-Lechon, M. J.; Groothuis, G. M.; Gustavsson, L.; Guyot, C.; Hallifax, D.; Hammad, S.; Hayward, A.; Haussinger, D.; Hellerbrand, C.; Hewitt, P.; Hoehme, S.; Holzhutter, H. G.; Houston, J. B.; Hrach, J.; Ito, K.; Jaeschke, H.; Keitel, V.; Kelm, J. M.; Kevin Park, B.; Kordes, C.; Kullak-Ublick, G. A.; LeCluyse, E. L.; Lu, P.; Luebke-Wheeler, J.; Lutz, A.; Maltman, D. J.; Matz-Soja, M.; McMullen, P.; Merfort, I.; Messner, S.; Meyer, C.; Mwinyi, J.; Naisbitt, D. J.; Nussler, A. K.; Olinga, P.; Pampaloni, F.; Pi, J.; Pluta, L.; Przyborski, S. A.; Ramachandran, A.; Rogiers, V.; Rowe, C.; Schelcher, C.; Schmich, K.; Schwarz, M.; Singh, B.; Stelzer, E. H.; Stieger, B.; Stober, R.; Sugiyama, Y.; Tetta, C.; Thasler, W. E.; Vanhaecke, T.; Vinken, M.; Weiss, T. S.; Widera, A.; Woods, C. G.; Xu, J. J.; Yarborough, K. M.; Hengstler, J. G. Recent advances in 2D and 3D in vitro systems using primary hepatocytes, alternative hepatocyte sources and non-parenchymal liver cells and their use in investigating mechanisms of hepatotoxicity, cell signaling and ADME. *Arch. Toxicol.* **2013**, *87* (8), 1315−530.

(3) Soldatow, V. Y.; Lecluyse, E. L.; Griffith, L. G.; Rusyn, I. Models for liver toxicity testing. *Toxicol. Res. (Cambridge, U. K.)* **2013**, *2* (1), 23−39.

(4) Wu, X. B.; Tao, R. Hepatocyte differentiation of mesenchymal stem cells. *Hepatobiliary Pancreatic Dis. Int.* **2012**, *11* (4), 360−71.

(5) Banas, A.; Yamamoto, Y.; Teratani, T.; Ochiya, T. Stem cell plasticity: learning from hepatogenic differentiation strategies. *Dev. Dyn.* **2007**, *236* (12), 3228−41.

(6) Rambhatla, L.; Chiu, C. P.; Kundu, P.; Peng, Y.; Carpenter, M. K. Generation of hepatocyte-like cells from human embryonic stem cells. *Cell Transplant.* **2003**, *12* (1), 1−11.

(7) Keller, G. Embryonic stem cell differentiation: emergence of a new era in biology and medicine. *Genes Dev.* **2005**, *19* (10), 1129−55.

(8) Schwartz, R. E.; Fleming, H. E.; Khetani, S. R.; Bhatia, S. N. Pluripotent stem cell-derived hepatocyte-like cells. *Biotechnol. Adv.* **2014**, *32* (2), 504−13.

(9) Talens-Visconti, R.; Bonora, A.; Jover, R.; Mirabet, V.; Carbonell, F.; Castell, J. V.; Gomez-Lechon, M. J. Hepatogenic differentiation of human mesenchymal stem cells from adipose tissue in comparison with bone marrow mesenchymal stem cells. *World J. Gastroenterol.* **2006**, *12* (36), 5834−45.

(10) Kern, S.; Eichler, H.; Stoeve, J.; Kluter, H.; Bieback, K. Comparative analysis of mesenchymal stem cells from bone marrow, umbilical cord blood, or adipose tissue. *Stem Cells* **2006**, *24* (5), 1294−301.

(11) Ishikawa, T.; Banas, A.; Hagiwara, K.; Iwaguro, H.; Ochiya, T. Stem cells for hepatic regeneration: the role of adipose tissue derived mesenchymal stem cells. *Curr. Stem Cell Res. Ther.* **2010**, *5* (2), 182−9.

(12) Lue, J.; Lin, G.; Ning, H.; Xiong, A.; Lin, C. S.; Glenn, J. S. Transdifferentiation of adipose-derived stem cells into hepatocytes: a new approach. *Liver Int.* **2010**, *30* (6), 913−22.

(13) Xu, D.; Nishimura, T.; Zheng, M.; Wu, M.; Su, H.; Sato, N.; Lee, G.; Michie, S.; Glenn, J.; Peltz, G. Enabling autologous human liver regeneration with differentiated adipocyte stem cells. *Cell Transplant.* **2014**, *23* (12), 1573−84.

(14) Banas, A.; Teratani, T.; Yamamoto, Y.; Tokuhara, M.; Takeshita, F.; Quinn, G.; Okochi, H.; Ochiya, T. Adipose tissue-derived mesenchymal stem cells as a source of human hepatocytes. *Hepatology* **2007**, *46* (1), 219−28.

(15) Engler, A. J.; Sen, S.; Sweeney, H. L.; Discher, D. E. Matrix elasticity directs stem cell lineage specification. *Cell* **2006**, *126* (4), 677−689.

(16) Ayala, R.; Zhang, C.; Yang, D.; Hwang, Y.; Aung, A.; Shroff, S. S.; Arce, F. T.; Lal, R.; Arya, G.; Varghese, S. Engineering the cell−material interface for controlling stem cell adhesion, migration, and differentiation. *Biomaterials* **2011**, *32* (15), 3700−3711.

(17) Teo, B. K. K.; Ankam, S.; Chan, L. Y.; Yim, E. K. F. Nanotopography/mechanical induction of stem-cell differentiation. In *Methods in Cell Biology*; Shivashankar, G. V., Ed.; Academic Press,

DOI: 10.1021/acsbiomaterials.6b00487
ACS Biomater. Sci. Eng. 2016, 2, 2255−2265

2010; Vol. *98*, Chapter 11, pp 241−294. DOI: 10.1016/S0091-679X(10)98011-4.
(18) Pittenger, M. F.; Mackay, A. M.; Beck, S. C.; Jaiswal, R. K.; Douglas, R.; Mosca, J. D.; Moorman, M. A.; Simonetti, D. W.; Craig, S.; Marshak, D. R. Multilineage potential of adult human mesenchymal stem cells. *Science* **1999**, *284* (5411), 143−147.
(19) Heng, B. C.; Yu, H.; Yin, Y.; Lim, S. G.; Cao, T. Factors influencing stem cell differentiation into the hepatic lineage in vitro. *J. Gastroenterol. Hepatol.* **2005**, *20* (7), 975−87.
(20) Yao, R.; Wang, J.; Li, X.; Da, J.; Qi, H.; Kee, K. K.; Du, Y. Hepatic differentiation of human embryonic stem cells as microscaled multilayered colonies leading to enhanced homogeneity and maturation. *Small* **2014**, *10* (21), 4311−4323.
(21) Gieseck, R. L., III; Hannan, N. R.; Bort, R.; Hanley, N. A.; Drake, R. A.; Cameron, G. W.; Wynn, T. A.; Vallier, L. Maturation of induced pluripotent stem cell derived hepatocytes by 3D-culture. *PLoS One* **2014**, *9* (1), e86372.
(22) Kim, J. H.; Jang, Y. J.; An, S. Y.; Son, J.; Lee, J.; Lee, G.; Park, J. Y.; Park, H. J.; Hwang, D. Y.; Kim, J. H.; Han, J. Enhanced metabolizing activity of human ES cell-derived hepatocytes using a 3D culture system with repeated exposures to xenobiotics. *Toxicol. Sci.* **2015**, *147* (1), 190−206.
(23) Kazemnejad, S.; Allameh, A.; Soleimani, M.; Gharehbaghian, A.; Mohammadi, Y.; Amirizadeh, N.; Jazayery, M. Biochemical and molecular characterization of hepatocyte-like cells derived from human bone marrow mesenchymal stem cells on a novel three-dimensional biocompatible nanofibrous scaffold. *J. Gastroenterol. Hepatol.* **2009**, *24* (2), 278−87.
(24) Cameron, K.; Tan, R.; Schmidt-Heck, W.; Campos, G.; Lyall, M. J.; Wang, Y.; Lucendo-Villarin, B.; Szkolnicka, D.; Bates, N.; Kimber, S. J.; Hengstler, J. G.; Godoy, P.; Forbes, S. J.; Hay, D. C. Recombinant laminins drive the differentiation and self-organization of hESC-derived hepatocytes. *Stem Cell Rep.* **2015**, *5* (6), 1250−62.
(25) Ghodsizadeh, A.; Hosseinkhani, H.; Piryaei, A.; Pournasr, B.; Najarasl, M.; Hiraoka, Y.; Baharvand, H. Galactosylated collagen matrix enhanced in vitro maturation of human embryonic stem cell-derived hepatocyte-like cells. *Biotechnol. Lett.* **2014**, *36* (5), 1095−106.
(26) Nagamoto, Y.; Tashiro, K.; Takayama, K.; Ohashi, K.; Kawabata, K.; Sakurai, F.; Tachibana, M.; Hayakawa, T.; Furue, M. K.; Mizuguchi, H. The promotion of hepatic maturation of human pluripotent stem cells in 3D co-culture using type I collagen and Swiss 3T3 cell sheets. *Biomaterials* **2012**, *33* (18), 4526−34.
(27) Baertschiger, R. M.; Serre-Beinier, V.; Morel, P.; Bosco, D.; Peyrou, M.; Clement, S.; Sgroi, A.; Kaelin, A.; Buhler, L. H.; Gonelle-Gispert, C. Fibrogenic potential of human multipotent mesenchymal stromal cells in injured liver. *PLoS One* **2009**, *4* (8), e6657.
(28) Qihao, Z.; Xigu, C.; Guanghui, C.; Weiwei, Z. Spheroid formation and differentiation into hepatocyte-like cells of rat mesenchymal stem cell induced by co-culture with liver cells. *DNA Cell Biol.* **2007**, *26* (7), 497−503.
(29) Soto-Gutierrez, A.; Navarro-Alvarez, N.; Zhao, D.; Rivas-Carrillo, J. D.; Lebkowski, J.; Tanaka, N.; Fox, I. J.; Kobayashi, N. Differentiation of mouse embryonic stem cells to hepatocyte-like cells by co-culture with human liver nonparenchymal cell lines. *Nat. Protoc.* **2007**, *2* (2), 347−56.
(30) Kim, M. H.; Kumar, S. K.; Shirahama, H.; Seo, J.; Lee, J. H.; Zhdanov, V. P.; Cho, N. J. Biofunctionalized hydrogel microscaffolds promote 3D hepatic sheet morphology. *Macromol. Biosci.* **2016**, *16* (3), 314−21.
(31) Erat, M. C.; Sladek, B.; Campbell, I. D.; Vakonakis, I. Structural analysis of collagen type I interactions with human fibronectin reveals a cooperative binding mode. *J. Biol. Chem.* **2013**, *288* (24), 17441−50.
(32) Lee, J. H.; Kim, H. J.; Kim, H.; Lee, S. J.; Gye, M. C. In vitro spermatogenesis by three-dimensional culture of rat testicular cells in collagen gel matrix. *Biomaterials* **2006**, *27* (14), 2845−53.
(33) Rozen, S.; Skaletsky, H. Primer3 on the WWW for general users and for biologist programmers. *Bioinformatics Methods and Protocols*; Methods in Molecular Biology 132; Springer, 2000; Vol. *132*, pp 365−386.10.1385/1-59259-192-2:365
(34) Kim, M. H.; Kumar, S. K.; Shirahama, H.; Seo, J.; Lee, J. H.; Cho, N.-J. Phenotypic regulation of liver cells in a biofunctionalized three-dimensional hydrogel platform. *Integr. Biol.* **2016**, *8*, 156−166.
(35) Lee, K. D.; Kuo, T. K.; Whang-Peng, J.; Chung, Y. F.; Lin, C. T.; Chou, S. H.; Chen, J. R.; Chen, Y. P.; Lee, O. K. In vitro hepatic differentiation of human mesenchymal stem cells. *Hepatology* **2004**, *40* (6), 1275−84.
(36) Talens-Visconti, R.; Bonora, A.; Jover, R.; Mirabet, V.; Carbonell, F.; Castell, J. V.; Gomez-Lechon, M. J. Human mesenchymal stem cells from adipose tissue: differentiation into hepatic lineage. *Toxicol. In Vitro* **2007**, *21* (2), 324−9.
(37) Petit, V.; Thiery, J. P. Focal adhesions: structure and dynamics. *Biol. Cell* **2000**, *92* (7), 477−94.
(38) Cukierman, E.; Pankov, R.; Stevens, D. R.; Yamada, K. M. Taking cell-matrix adhesions to the third dimension. *Science* **2001**, *294* (5547), 1708−1712.
(39) Harunaga, J. S.; Yamada, K. M. Cell-matrix adhesions in 3D. *Matrix Biol.* **2011**, *30* (7−8), 363−8.
(40) Chang, T. T.; Hughes-Fulford, M. Monolayer and spheroid culture of human liver hepatocellular carcinoma cell line cells demonstrate distinct global gene expression patterns and functional phenotypes. *Tissue Eng., Part A* **2009**, *15* (3), 559−67.
(41) Selden, C.; Khalil, M.; Hodgson, H. Three dimensional culture upregulates extracellular matrix protein expression in human liver cell lines–a step towards mimicking the liver in vivo? *Int. J. Artif. Organs* **2000**, *23* (11), 774−81 http://www.ncbi.nlm.nih.gov/pubmed/11132022.
(42) Ghosh, S.; Spagnoli, G. C.; Martin, I.; Ploegert, S.; Demougin, P.; Heberer, M.; Reschner, A. Three-dimensional culture of melanoma cells profoundly affects gene expression profile: a high density oligonucleotide array study. *J. Cell. Physiol.* **2005**, *204* (2), 522−31.
(43) Lendahl, U.; Zimmerman, L. B.; McKay, R. D. G. CNS stem cells express a new class of intermediate filament protein. *Cell* **1990**, *60* (4), 585−595.
(44) Lau, T. T.; Ho, L. W.; Wang, D. A. Hepatogenesis of murine induced pluripotent stem cells in 3D micro-cavitary hydrogel system for liver regeneration. *Biomaterials* **2013**, *34* (28), 6659−69.
(45) Dunn, J. C. Y.; Yarmush, M. L.; Koebe, H. G.; Tompkins, R. G. Hepatocyte function and extracellular-matrix geometry - long-term culture in a sandwich configuration. *FASEB J.* **1989**, *3* (2), 174−177 http://www.fasebj.org/content/3/2/174.abstract.
(46) Berger, D. R.; Ware, B. R.; Davidson, M. D.; Allsup, S. R.; Khetani, S. R. Enhancing the functional maturity of induced pluripotent stem cell-derived human hepatocytes by controlled presentation of cell-cell interactions in vitro. *Hepatology* **2015**, *61* (4), 1370−81.
(47) Adams, J. C.; Watt, F. M. Regulation of development and differentiation by the extracellular matrix. *Development* **1993**, *117* (4), 1183−1198 http://dev.biologists.org/content/117/4/1183.
(48) Martinez-Hernandez, A.; Amenta, P. S. The hepatic extracellular matrix. I. Components and distribution in normal liver. *Virchows Arch. A: Pathol. Anat. Histopathol.* **1993**, *423* (1), 1−11.
(49) Martinez-Hernandez, A. The hepatic extracellular matrix. I. Electron immunohistochemical studies in normal rat liver. *Lab. Invest.* **1984**, *51* (1), 57−74 http://www.ncbi.nlm.nih.gov/pubmed/6376944.
(50) Sawada, N.; Tomomura, A.; Sattler, C. A.; Sattler, G. L.; Kleinman, H. K.; Pitot, H. C. Extracellular-matrix components influence DNA-synthesis of rat hepatocytes in primary culture. *Exp. Cell Res.* **1986**, *167* (2), 458−470.
(51) Sanchez, A.; Alvarez, A. M.; Pagan, R.; Roncero, C.; Vilaro, S.; Benito, M.; Fabregat, I. Fibronectin regulates morphology, cell organization and gene expression of rat fetal hepatocytes in primary culture. *J. Hepatol.* **2000**, *32* (2), 242−50.

DOI: 10.1021/acsbiomaterials.6b00487
ACS Biomater. Sci. Eng. 2016, 2, 2255−2265